# Spatially segregated control of $Ca^{2+}$ release in developing skeletal muscle of mice

Natalia Shirokova, Roman Shirokov, Daniela Rossi*, Adom González, Wolfgang G. Kirsch, Jesús García†, Vincenzo Sorrentino*‡ and Eduardo Ríos

*Department of Molecular Biophysics and Physiology, Rush University, 1750 W. Harrison Street, Chicago, IL 60612, USA, †Department of Physiology and Biophysics, University of Illinois at Chicago, 900 S. Ashland Avenue, Chicago, IL 60607, USA, *Department of Biomedical Sciences, University of Siena, I-53100 Siena, Italy and ‡DIBIT, San Raffaele Scientific Institute, I-20132 Milan, Italy*

(Received 26 July 1999; accepted after revision 7 September 1999)

1. Confocal laser scanning microscopy was used to monitor $Ca^{2+}$ signals in primary-cultured myotubes, prepared from forelimbs of wild-type or ryanodine receptor type 3 (RyR3) knockout mice. Myotubes loaded with the acetoxymethyl ester (AM) form of fluo-3 were imaged at rest or under whole-cell patch clamp.

2. Discrete $Ca^{2+}$ release events were detected in intact wild-type and RyR3-knockout myotubes. They showed almost no difference in amplitude and width, but were substantially different in duration. In wild-type myotubes (660 events, 57 cells) the amplitude was 1·27 (0·85, 1·97) (median (25%, 75%)) units of resting fluorescence, the full width at half-magnitude (FWHM) was 1·4 (0·9, 2·3) $\mu$m, and the full duration at half-magnitude (FDHM) was 25·3 (9·6, 51·7) ms. In RyR3-knockout myotubes (655 events, 83 cells) the amplitude was 1·30 (0·84, 2·08), FWHM was 1·63 (1·02, 2·66) $\mu$m, and FDHM was 43·6 (23·6, 76·9) ms.

3. Depolarization under voltage clamp of both wild-type and RyR3-knockout myotubes produced substantial $Ca^{2+}$ release devoid of discrete $Ca^{2+}$ events. Discrete events were still present but occurred without correlation with the applied pulse, largely at locations where the pulse did not elicit release.

4. The local correspondence between voltage control and absence of discrete events implies that the functional interaction with voltage sensors suppresses the mechanism that activates discrete events. Because it applies whether RyR3 is present or not, it is this exclusion by voltage of other control mechanisms, rather than isoform composition, that primarily determines the absence of discrete $Ca^{2+}$ events in adult mammalian muscle.

In skeletal muscle, a key step of excitation–contraction coupling (ECC) is the transduction of the depolarization sensed by membrane voltage sensors (dihydropyridine receptors, DHPRs) to opening of the sarcoplasmic reticulum (SR) $Ca^{2+}$ channels (ryanodine receptors, RyRs), resulting in $Ca^{2+}$ release and contractile activation. In amphibian skeletal muscle most $Ca^{2+}$ release occurs as $Ca^{2+}$ sparks (Tsugorka *et al.* 1995; Klein *et al.* 1996), a term used to describe both discrete packets of release and the highly localized elevations of $[Ca^{2+}]$ and indicator fluorescence that they produce (Cheng *et al.* 1993). These sparks are probably activated by $Ca^{2+}$ (Klein *et al.* 1996; Shirokova & Ríos, 1997) in a manifestation of $Ca^{2+}$-induced $Ca^{2+}$ release (CICR; Endo, 1977; Fabiato, 1984). A second, continuous form of release was also demonstrated in frog skeletal muscle. This form of release was proposed to be activated directly by mechanical interaction with membrane voltage sensors and to provide trigger $Ca^{2+}$ for activation of $Ca^{2+}$ sparks (Shirokova & Ríos, 1997).

In adult mammalian skeletal muscle no $Ca^{2+}$ sparks were detected under the experimental conditions that produced them in frogs (Shirokova *et al.* 1998), a diffuse release being observed instead. However, spontaneous $Ca^{2+}$ sparks were abundant in mice myotubes in primary culture (Shirokova *et al.* 1998). This intriguing difference between taxonomic classes motivated the present study.

Skeletal muscle contains different isoforms of RyR. Non-mammalian vertebrates express two skeletal muscle RyR isoforms, termed $\alpha$ and $\beta$ (reviewed by Sutko & Airey, 1996; Ogawa *et al.* 1999), which are present in equal amounts in amphibian skeletal muscle. Adult mammalian skeletal muscle expresses predominantly RyR1 (Marks *et al.* 1989; Takeshima *et al.* 1989), the mammalian homologue of the

α isoform (Murayama & Ogawa, 1992), while expression of RyR3 (homologous to β RyR) is substantial in developing muscle (Tarroni *et al.* 1997). It was suggested that RyR3 (or β) is better suited than RyR1 (or α) to be controlled by $Ca^{2+}$ (Percival *et al.* 1994).

Based on the absence of sparks in adult rat muscle, we have suggested that RyR3 or β isoforms are required for the production of $Ca^{2+}$ sparks in skeletal muscle (Shirokova *et al.* 1998). Here we test the hypothesis by characterizing and comparing local properties of $Ca^{2+}$ release in cultured myotubes from wild-type and RyR3-knockout mice.

## METHODS

### Cell culture and solutions

Experiments were carried out on mammalian muscle cultures (myotubes) prepared from wild-type or RyR3-knockout mice (Bertocchini *et al.* 1997). Newborn mice were anaesthetized with halothane and decapitated as approved by the American Veterinary Medical Association. The forelimbs were removed and then minced with scissors in $Ca^{2+}$-free rodent Ringer solution (Beam & Knudson, 1988). They were incubated with trypsin Type XI (Sigma, Inc., St Louis, MO, USA, 3 mg $ml^{-1}$) and DNase I (Sigma, 0·01 mg $ml^{-1}$) for 30 min at 37 °C. Dissociated muscles were triturated with a Pasteur pipette in growth medium (v/v, 80% Dulbecco's modified Eagle's medium (DMEM), 10% horse serum and 10% fetal bovine serum (all from Gibco, Inc., Gaithesburg, MD, USA) with 4·5 g $l^{-1}$ glucose) to obtain a suspension of myoblasts. After passing the suspension through a 250 μm nylon filter, the cells were centrifuged, resuspended in growth medium and plated on collagen-coated glass coverslips. After 48 h differentiation medium was substituted (98% DMEM, 2% horse serum with 4·5 g $l^{-1}$ glucose). Experiments were carried out after 3 to 10 days in this medium, and at room temperature (~20 °C).

Myotubes were imaged in 2 mM $Ca^{2+}$ external solution (composition: 2 mM $CaCl_2$, 2 mM $MgCl_2$, 150 mM $TEACH_3SO_3$, 10 mM Hepes, 1 μM TTX) after incubation for 20 min in rodent Ringer solution containing the acetoxymethyl ester (AM) form of fluo-3 (10 μM; Molecular Probes, Inc., Eugene, OR, USA). In voltage clamp experiments the cells, preloaded with fluo-3 AM, were patched with pipettes containing: 130 mM caesium glutamate, 20 mM CsCl, 2 mM EGTA, 5 mM MgATP, 10 mM glucose, 5 mM phosphocreatine, and $Ca^{2+}$ added to a nominal free concentration of 100 nM. All solutions were adjusted to 300–320 mosmol $kg^{-1}$ and pH 7·2.

### Electrophysiological and optical measurements

Cells were voltage clamped in the standard whole-cell patch clamp configuration using an Axopatch 200B amplifier (Axon Instruments Inc., Foster City, CA, USA) and 16 bit A/D–D/A converter card (HSDAS 16; Analogic Corp., Peabody, MA, USA) on a PC. Patch electrodes were pulled from Corning 7052 glass and had resistances of 1·0–1·5 MΩ.

Cells were imaged with MRC-1000 (Bio-Rad, Hercules, CA, USA) equipped with a ×40 water immersion objective lens (Zeiss, Inc., Oberköchen, Germany), and used in standard fluo-3 mode (Shirokova & Ríos, 1997). Images representing the scanned intensity of fluorescence $F(x,t)$, as a function of position along the scanned line ($x$) and time ($t$), were formed by collections of 768 intensity values taken at 0·166 μm distances and repeated every 2 or 4·3 ms. Unless otherwise specified, images shown are of $F(x,t)/F_0(x)$, fluorescence intensity normalized to a baseline intensity $F_0(x)$, obtained by averaging $F_0(x,t)$ over the time when no events were detected. Discrete events were automatically detected and measured by a recently described procedure (Cheng *et al.* 1999), which detects all increases in fluorescence relative to a suitable global baseline that satisfy a threshold criterion. This threshold, which in the present case was 2 standard deviations of $F/F_0$ in the surrounding 20 μm region, is applied to a spatially filtered version of the image. Then the morphological parameters of the events detected are measured on the unfiltered normalized image as follows: amplitude, defined as peak minus local baseline averaged for 50 ms before the event; full width at half-magnitude (FWHM or spatial width), the extent of the region where separation from the local baseline is above half-amplitude at the time of the peak; full duration at half-magnitude (FDHM, or 'duration'), the time during which $F/F_0$ averaged at the three central pixels is above half-amplitude; and rise time, elapsed between 10% and peak of $F/F_0$, measured on the average of the cubic spline interpolate of the time course in three central pixels (because this procedure nominally increases the temporal resolution of the measure, rise times are given with a precision of 0·1 ms).

### Immunofluorescence staining

Cells attached to coverslips were washed twice with phosphate-buffered saline (PBS), and fixed in precooled (−20 °C) methanol/acetone (1:1) for 5–10 min at 4 °C. Fixed myotubes were incubated overnight at 4 °C in labelling buffer (1% bovine serum albumin, 2% normal goat serum in PBS) to block non-specific binding. The labelling buffer contained diluted primary antibodies (anti-RyR1 or anti-RyR3; Tarroni *et al.* 1997). Then cells were incubated with FITC-conjugated secondary antibodies (Sigma) for 1 h at room temperature. Coverslips were mounted on slides and imaged with the confocal microscope.

## RESULTS

Firstly, we describe and quantify 'spontaneous' events observed in wild-type myotubes, and show evidence that discrete increases in $[Ca^{2+}]$ spatially propagate, therefore involving multiple sources. Secondly, we show that discrete events also occur in RyR3-knockout myotubes, and compare them quantitatively with those observed in wild-type cells. Thirdly, we compare the spontaneous events with the signals of $Ca^{2+}$ release elicited by voltage clamp pulses, demonstrating an unexpected segregation of these two forms of release.

### Spontaneous $Ca^{2+}$ release events in wild-type myotubes

After 3–5 days in differentiation media, most myotubes became long and multinucleated. Immunostaining demonstrated the presence of both RyR1 and RyR3 in wild-type myotubes (Fig. 1*A*). The distribution pattern of RyR1- and RyR3-immunoreactive clusters changed over time in a characteristic manner, similar to that reported by Flucher *et al.* (1994). After 3–5 days most myotubes showed polymorphic clusters of RyR1 and RyR3 throughout the cytoplasm (Fig. 1*Ac*). As the culture aged, the density of clusters increased and the distribution became more regular. After 7 days most wild-type myotubes exhibited a double beaded RyR1 and RyR3 staining pattern, consistent with the formation of an elaborate T tubular network and

incorporation of both RyR isoforms into T tubule–SR junctions (Fig. 1*Aa* and *b*).

In resting intact myotubes discrete events of $Ca^{2+}$-related fluorescence were present with widely variable amplitudes, widths and durations. An automatic computer procedure (Cheng *et al.* 1999 and Methods) located the events and measured their morphological parameters. Figure 1*B* shows examples of events of different morphology. Figure 1*Ba* shows several events similar to $Ca^{2+}$ sparks from mammalian heart and frog skeletal muscle. In Fig. 1*Bb* and *c* events with greater amplitudes, widths and durations are shown. The plots represent $F/F_0$, averaged spatially over 2·5 $\mu$m-wide bands centred at the arrowheads.

The distribution of morphological parameters of 660 events in 57 cells is represented in Fig. 1*C*. Because the distributions were skewed three quartiles are given for each measurement: median (25%, 75%). The amplitude, normalized to resting fluorescence, was 1·27 (0·85, 1·97), FWHM was 1·40 (0·9, 2·3) $\mu$m, and FDHM was 25·3 (9·6, 51·7) ms. Contained in the broad and skewed distribution of spatial width are events up to 10 times wider than those produced by mathematical simulation using point or small-size sources (e.g. Smith *et al.* 1997; Ríos *et al.* 1999), a good indication of their origin at multiple, separate sources of $Ca^{2+}$ release.

### Events in the presence of caffeine

In adult muscle, caffeine is an enhancer of $Ca^{2+}$ sparks (Klein *et al.* 1996; González *et al.* 1999) whose effect is understood, at least in part, as an increase in sensitivity of channels to activation by $Ca^{2+}$ (Rousseau *et al.* 1988; Herrmann-Frank *et al.* 1999). Caffeine was used in the present study, at 0·5–1 mM, for the dual purpose of increasing event frequency and probing mechanism.

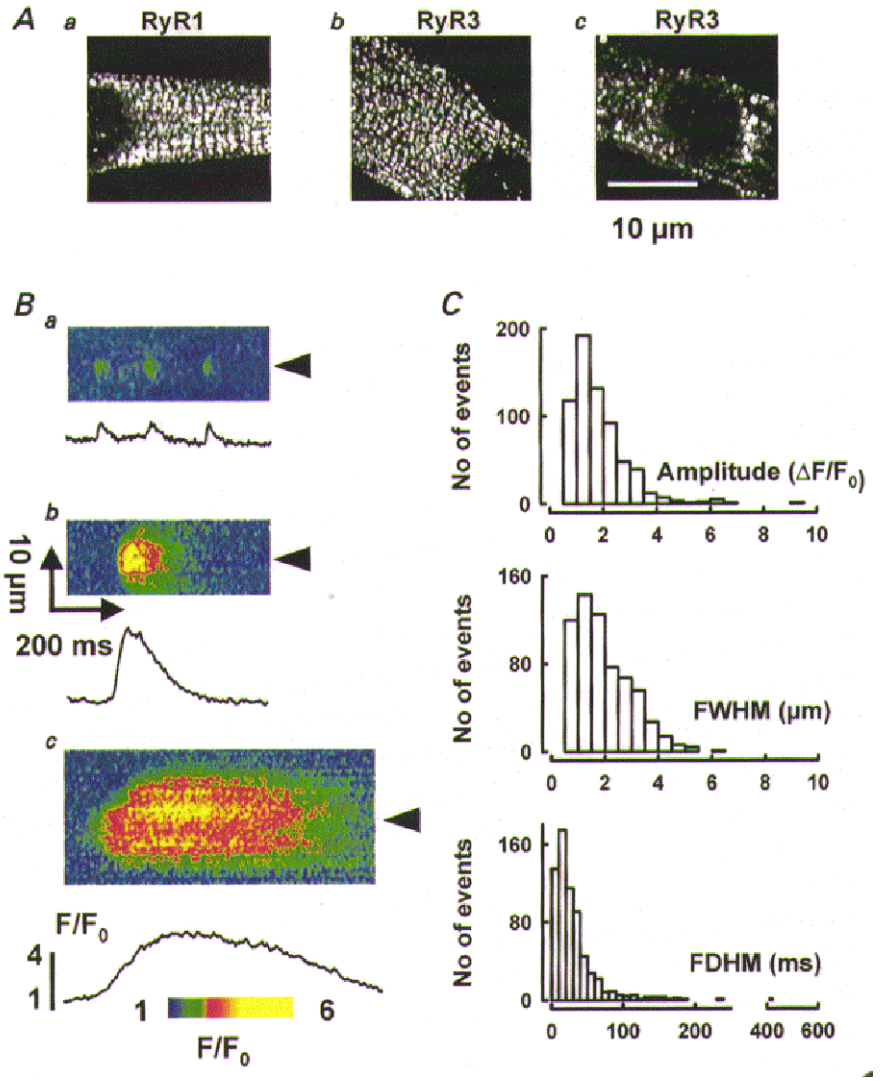


**Figure 1. Discrete events of $Ca^{2+}$ release in wild-type myotubes**

*A*, immunolocalization of RyR1 (*a*) and RyR3 (*b* and *c*) in wild-type cells. *B*, line-scan images of normalized fluorescence with discrete events of $Ca^{2+}$ release, illustrating a variety of amplitudes (from as little as 0·95 in *a* to 3·3 in *b*), spatial widths (from 0·71 to 6·3 $\mu$m) and durations (from 12 to 510 ms). *C*, histograms of amplitude, spatial width and duration, for 660 events detected in 57 cells as described in Methods.

Caffeine increased event frequency from an average of $3{\cdot}5 \times 10^{-3}$ $\mu m^{-1} s^{-1}$ in reference to between 7·5 and $28 \times 10^{-3}$ $\mu m^{-1} s^{-1}$ (depending on dose and individual experiment). At the increased frequency, there were many examples of event propagation, either around or away from an initial focus. Figure 2*Aa* is a two-dimensional (or (*x*,*y*)) image of fluorescence with three events (marked by arrowheads) that occurred close in time at different locations in the myotube. Figure 2*Ab* and *c* shows two line-scan images acquired sequentially at the line indicated in Fig. 2*Aa*. Events with radically different morphology can be observed, including fast-rising and spatially narrow events (examples in Fig. 2*Ac*), wider and longer-lasting events of larger amplitude, and occasionally a slow $Ca^{2+}$ wave. The overall scarcity of events in this cell ($7{\cdot}5 \times 10^{-3}$ $\mu m^{-1} s^{-1}$) suggests that those in Fig. 2*Ab* and *c* originate at the same hyperactive channel or cluster, and occasionally propagate to other channels in the surroundings.

Figure 2*B* shows more examples of propagating release involving smaller foci. Events of complex shape that appear repetitively in the line-scan of Fig. 2*Ba* are shown enlarged in *Bb* and *c*. In them the boundaries between regions of low and elevated fluorescence are linear, with the same slope, which is consistent with propagation away from the origin, at a constant speed of about 80 $\mu m\ s^{-1}$. Figure 2*Bd* and *e* shows examples obtained from another cell scanned along the same line. It is believed that in muscle $Ca^{2+}$ mediates propagation of spontaneous events and waves (Cheng *et al.* 1996; Parker *et al.* 1996; Wier *et al.* 1997; Blatter *et al.* 1997). In all the examples shown here [$Ca^{2+}$] was increased above resting level along the propagation path. This, and the fact that propagation was enhanced by caffeine, are concurrent with the idea that $Ca^{2+}$ is the mediator of propagation, hence the activator of these polymorphic 'spontaneous' events. Involvement of other mediators (Jaimovich & Liberona, 1997) or mechanisms involving dual mediators (i.e. Lechleiter & Clapham, 1992) cannot be ruled out.

### Spontaneous $Ca^{2+}$ release events in RyR3-knockout myotubes

Figure 3*A* illustrates immunolocalization tests of RyR1 and RyR3 in RyR3-knockout myotubes. The distribution pattern of RyR1 clusters changed over time in a manner similar to that in wild-type myotubes. While in young cells

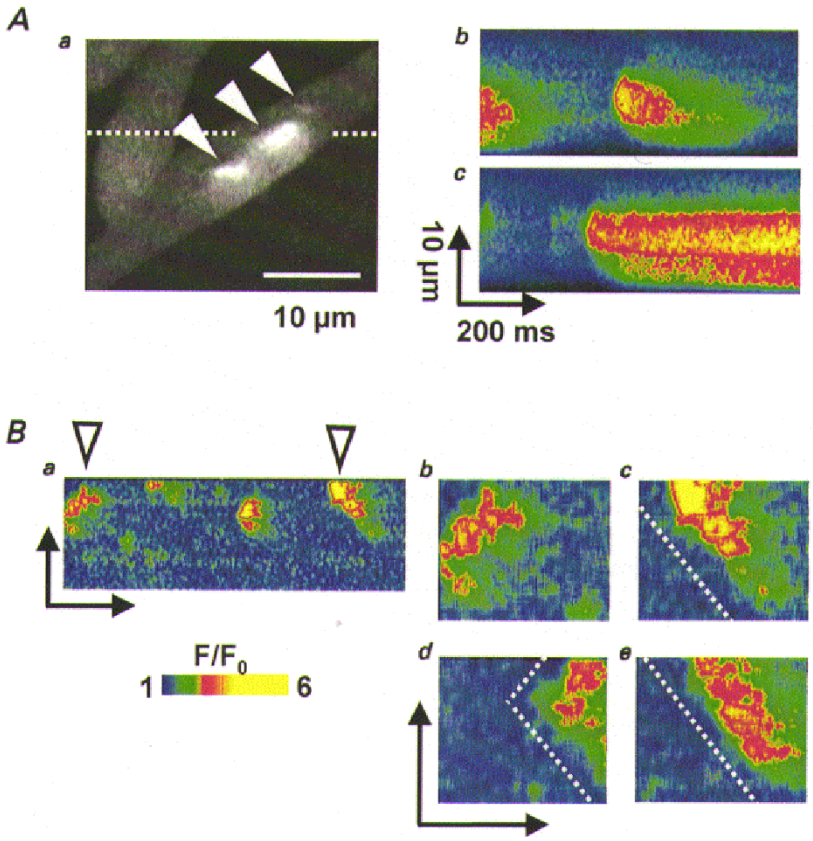


**Figure 2. Spontaneous $Ca^{2+}$ release activity enhanced by caffeine**

*A*, diversity of $Ca^{2+}$ events. *a*, two-dimensional scan image of fluorescence in a wild-type myotube exposed to 0·5 mM caffeine, with three $Ca^{2+}$ events having different spatial and temporal characteristics. *b* and *c*, line-scan images acquired sequentially along the line indicated in *a* with widely different events. *B*, examples of propagating events. *a*, line-scan image of a wild-type myotube exposed to caffeine. Images in *b* and *c* are enlargements of events in *a*, with dashed line parallel to propagation fronts. *d* and *e* are sequential line-scan images from another cell. The slope of propagation fronts is similar in different cells, consistent with a fixed speed of propagation.

RyR1 clusters were randomly distributed throughout the cytoplasm, in mature myotubes they formed double rows transversely to the cell's long axis (Fig. 3*Aa*). No RyR3-related immunofluorescence was ever detected (Fig. 3*Ab*).

Although at a frequency lower than in the wild-type, discrete events of $Ca^{2+}$ release with widely variable amplitude, width and duration were also observed in intact RyR3-knockout myotubes (Fig. 3*B*). Distributions of morphological parameters of 655 $Ca^{2+}$ events recorded in 83 cells are represented in Fig. 3*C*. The median amplitude (1·30 (0·84, 2·08)) and width (1·63 (1·02, 2·66)) $\mu$m of $Ca^{2+}$ release events in RyR3-knockout myotubes did not differ much from those of wild-type cells. Event durations, however, were significantly longer. Events lasting hundreds of milliseconds were much more frequent in RyR3-knockout cells, whereas events with FDHM less than 10 ms were absent. Figure 3*Bc* and *d* presents line-scan images of long-lasting $Ca^{2+}$ events (of 1·29 and 0·98 s duration, respectively). Differences are obvious in the inset of Fig. 3*C*, where FDHM histograms in wild-type (open bars) and RyR3-knockout cells (filled bars) are plotted in semi-logarithmic time scale. The median duration was 72% greater and the first quartile was 146% greater in RyR3-knockout myotubes (43·6 (23·6, 76·9) ms *vs.* 25·3 (9·6, 51·7) ms).

Approximately 5% of the events detected in RyR3-knockout cells had a FDHM of less than 20 ms. Such 'brief' events, defined here by an arbitrary duration boundary, are especially interesting regarding the postulated role of

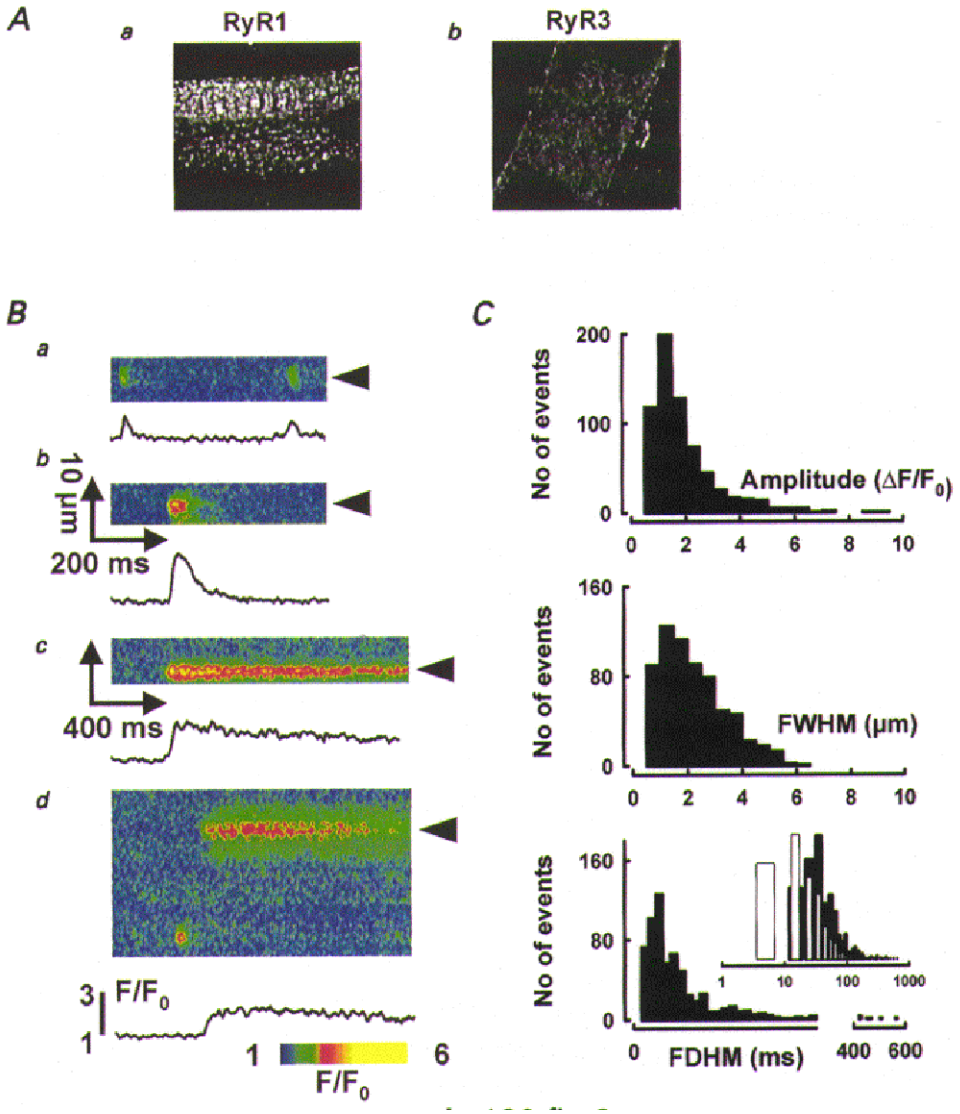


**Figure 3. Discrete events of $Ca^{2+}$ release in RyR3-knockout myotubes**

*A*, tests for immunolocalization of RyR1 (*a*) and RyR3 (*b*) in RyR3-knockout cells. Magnification as in Fig. 1*A*. *B*, line-scan images of $F/F_0$ in RyR3-knockout myotubes, showing discrete events in knockout cells. Traces plot time course of $F/F_0$ averaged as described for Fig. 1. The event amplitudes range from 1·1 (*a*) to 3·1 (*b*); FWHM from 2·5 (*a*) to 3·1 $\mu$m (*b*); and FDHM from 18 (*a*) to 1290 ms (*c*). *d* shows another example of a long-lasting event, recorded at 4·3 ms per line (FDHM, 980 ms). *C*, histograms of amplitude, width, and duration for 655 events detected in RyR3-knockout myotubes (83 cells). Inset, histogram of FDHM in wild-type (□) or RyR3-knockout cells (■), on a logarithmic time scale.

RyR3 in the generation of $Ca^{2+}$ sparks (Shirokova *et al.* 1998; Ward *et al.* 1999). Figures 3*Ba* and 4*A* and *B* show examples of brief events. Figure 4*Aa* and *Ba* shows line-scan images of fluorescence recorded in two different myotubes. Normalized fluorescence is shown in Fig. 4*Ab* and *Bb*, and under the images are plots of $F/F_0$ averaged over 1·35 $\mu$m bands centred at the arrowheads. The five events identified in the traces had a mean (± s.e.m.) amplitude of 1·97 ± 0·17, spatial width of 1·76 ± 0·20 $\mu$m, duration of 16·6 ± 1·17 ms, and rise time of 5·87 ± 0·62 ms. By comparison, the mean values from 5000 spontaneous events detected in 12 permeabilized adult frog semitendinosus muscle cells were, respectively, 1·92, 1·31 $\mu$m, 11·0 ms and 5·60 ms (A. González, W. Kirsch, G. Pizarro, N. Shirokova & E. Ríos, unpublished results).

The histograms in Fig. 4*C* compare morphological parameters of 37 brief events detected in RyR3-knockout cells with those of 87 events in wild-type cells. Although the distribution of FDHM was skewed toward longer durations in RyR3-knockout myotubes, other parameters appeared to be similar. Median amplitude was 1·25 (0·92, 1·81) in knockouts and 1·07 (0·81, 1·5) in the wild-type, width was 1·15 (0·77, 1·76) *vs.* 1·31 (0·86, 2·03) $\mu$m in the wild-type, while rise times were 5·5 (3·94, 8·2) *vs.* 4·3 (2·3, 7·5) ms. Events in this subset generally resemble $Ca^{2+}$ sparks of frog muscle.

In summary, the absence of RyR3 selectively increases the duration of spontaneous events. Brief events resembling sparks of adult muscle still occur, albeit less frequently.

### Voltage-activated $Ca^{2+}$ release in developing myotubes

$Ca^{2+}$ release could also be induced by voltage clamp depolarization. Initially, cells were loaded with fluo-3 AM and imaged. Only cells that exhibited spontaneous $Ca^{2+}$ events in resting conditions were voltage clamped (using a pipette with no $Ca^{2+}$ indicator). All measurements were made within 10–20 min after membrane rupture to minimize perfusion artifacts. Cells were scanned at locations

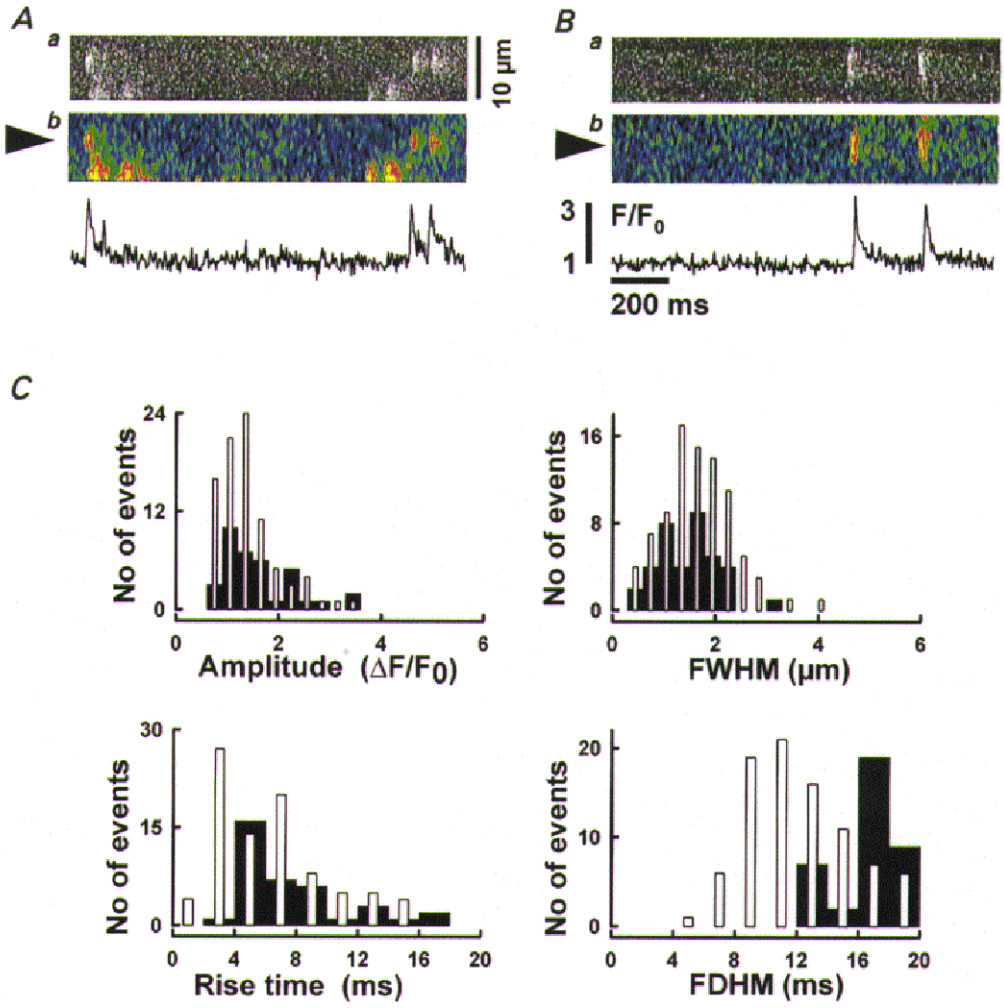


**Figure 4. $Ca^{2+}$ spark-like events in wild-type and RyR3-knockout myotubes**

*A* and *B*, brief $Ca^{2+}$ events in RyR3-knockout myotubes. Line-scan images of fluorescence (*a*) or $F/F_0$ (*b*) from different cells. Traces plot $F/F_0$ averaged spatially in 1·35 $\mu$m-wide bands centred at the arrowheads. Average parameter values for the five events included in these plots are given in the text. *C*, properties of brief $Ca^{2+}$ events, defined as having FDHM < 20 ms. Histograms of amplitude, width, rise and duration time for 87 events from wild-type cells (□) and 37 events from RyR3-knockout cells (■) are shown.

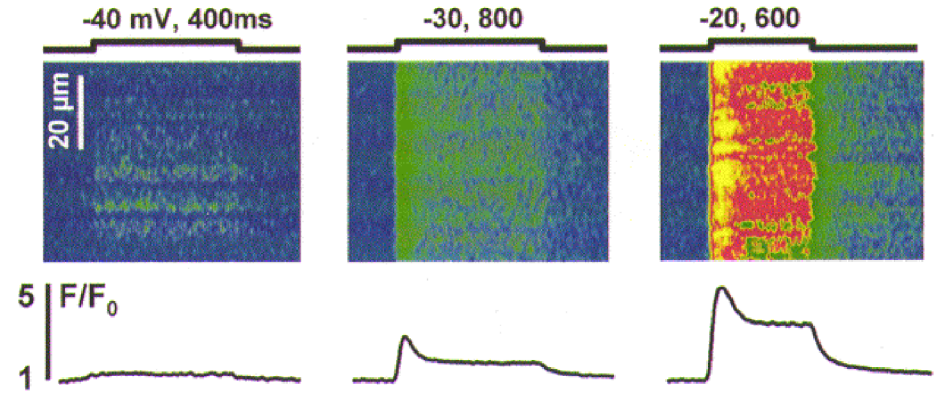


**Figure 5. Voltage-activated release in wild-type myotubes**

Line-scan images of $F/F_0$ in a myotube pulsed as indicated (mV, ms). The traces plot time course of spatially averaged $F/F_0$. Note different time scale of the image at −40 mV, corresponding to a faster scanning rate (2 *vs.* 4·3 ms per scan).

adjacent to the patch pipette. Some 20 voltage pulses were applied in a typical experiment.

Figure 5 illustrates representative $Ca^{2+}$ signals and their voltage dependence. At the top are line-scan images of normalized fluorescence in a wild-type myotube pulsed to the indicated voltages. The traces below are time courses of averaged normalized fluorescence. Depolarizations produced $Ca^{2+}$ release with a diffuse pattern similar to that observed in adult rat skeletal muscle (Shirokova *et al.* 1998). Even though discrete $Ca^{2+}$ events were present at rest, very few events were found upon depolarization at any voltage in 48 cells (including 36 wild-type and 11 RyR3-knockout myotubes).

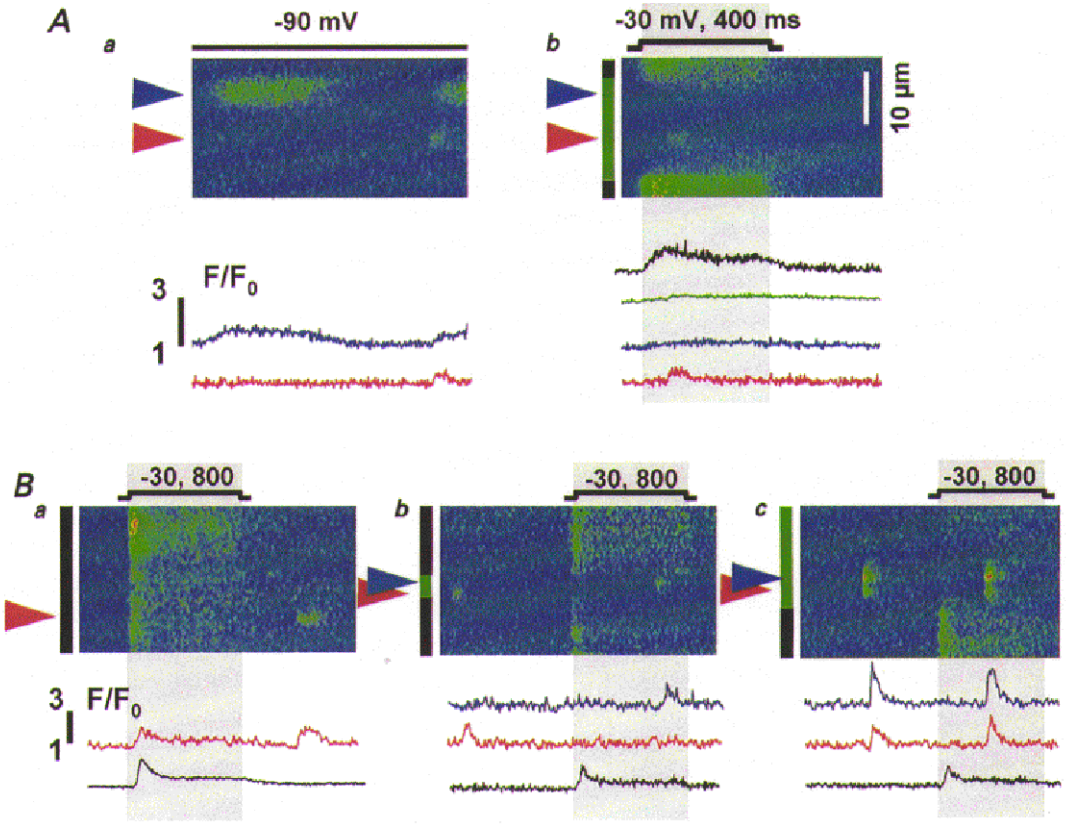


**Figure 6. Spatial segregation of two forms of $Ca^{2+}$ release in wild-type cells**

*A*, line-scan images of $F/F_0$ from the same myotube held at −90 mV (*a*) or depolarized as indicated (*b*). Arrowheads indicate locations where discrete events arose. The green bar in *b* marks the portion of the scanned region where voltage did not elicit $Ca^{2+}$ release and black bars the portions where it did. Traces represent normalized fluorescence averaged within the regions indicated by bars or in 2·5 $\mu$m-wide bands centred at the arrowheads, and are colour coded accordingly. *B*, images of normalized fluorescence obtained from another cell depolarized to −30 mV for 800 ms as indicated. Note the different time scales in *A* and *B*, corresponding to different scanning rates (2 *vs.* 4·3 ms per scan).

### Segregation of discrete $Ca^{2+}$ events from continuous voltage-induced release

In patch clamp experiments discrete $Ca^{2+}$ events were occasionally detected, but occurred without correlation with the applied pulse, generally at locations different from those that released $Ca^{2+}$ upon depolarization. Because the frequency of spontaneous events appeared to be greater in younger myotubes, the experiments described below were carried out in cells held for no more than 3 days in differentiation medium.

Figure 6*A* is from a wild-type myotube scanned along the same line while the cell was held at −90 mV (*a*) or depolarized as indicated (*b*). Discrete $Ca^{2+}$ events with different morphology occurred at two sites (marked by blue and red arrowheads). Blue and red traces are $F/F_0$ at the arrowheads (averaged spatially as before), with $F_0$ obtained from the resting period that precedes the pulse.

Depolarization produced release that was temporally continuous but spatially inhomogeneous. There was a silent region in the cell (indicated by the green bar before panel *Ab*), which did not produce $Ca^{2+}$ release in response to depolarizing pulses. The green trace is normalized fluorescence averaged within the region. (The creeping increase in fluorescence corresponds to a slow increase in global $Ca^{2+}$, produced by $Ca^{2+}$ releasing sites outside the region.) The region contains functional release sites, because discrete events occasionally arose in it (Fig. 6*Ab*). The occurrence of discrete events did not correlate with the applied pulses, and the region did not produce release upon four other subsequent depolarizations (not shown) at 1–2 min intervals. Therefore the absence of voltage-operated release is unlikely to be due to inactivation of $Ca^{2+}$ release units, and must correspond instead to a lack (or lack of function) of voltage sensing machinery within the region. Two other regions (black bars) generated continuous release upon depolarization (black trace in Fig. 6*Ab*). No discrete $Ca^{2+}$ events arose from them.

The above observations suggest a dissociation of voltage control and discrete release. To quantify them we compared the spatial frequency density ($f$) of discrete events (number of events per unit space and time) at locations that did not produce $Ca^{2+}$ release during depolarization ($f_{V\text{insensitive}}$) with that at locations that did release $Ca^{2+}$ upon depolarization ($f_{V\text{sensitive}}$). In this particular cell $f_{V\text{insensitive}}$ was $2{\cdot}63 \times 10^{-3}\ \mu m^{-1}\ s^{-1}$, whereas $f_{V\text{sensitive}}$ was 0, meaning that the two forms of release occurred at separate, mutually exclusive locations.

Other examples of spatial segregation of discrete events and voltage-operated continuous release are shown in Fig. 6*B*. The line-scan images were acquired at three different locations in another myotube, depolarized as indicated. Silent regions, which did not produce continuous release during depolarization, are seen in Fig. 6*Bb* and *c*. Discrete events occurred within these regions. Voltage-operated

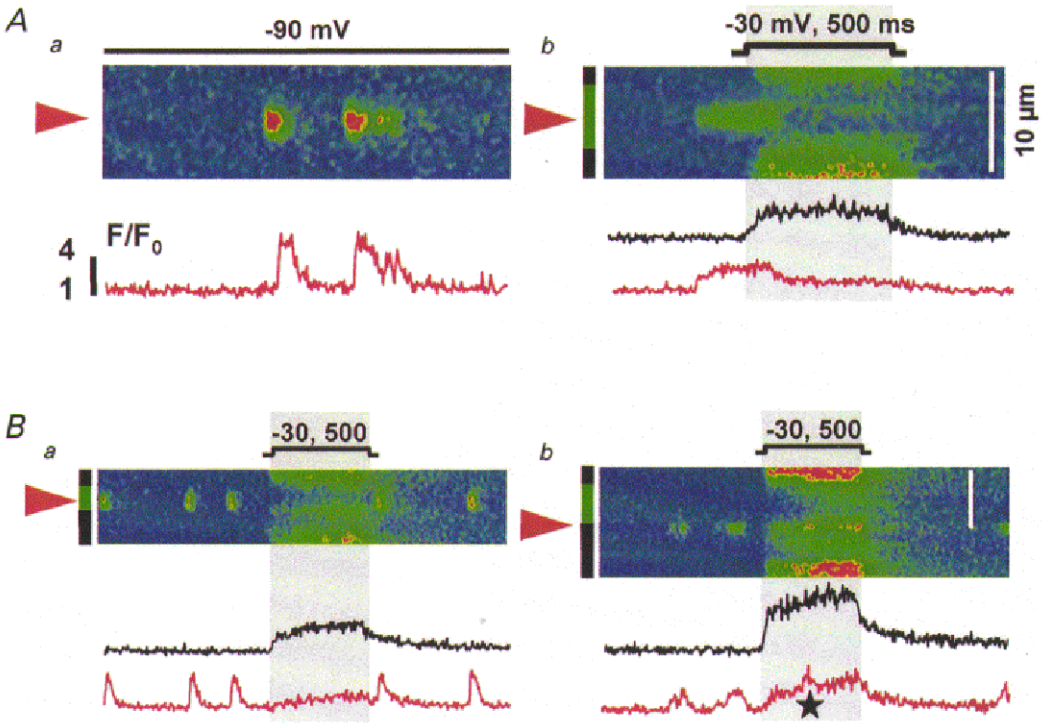


**Figure 7. Spatial segregation of two forms of $Ca^{2+}$ release in RyR3-knockout myotubes**

*A*, line-scan images from the same knockout myotube held at −90 mV (*a*) or depolarized as indicated (*b*). *B*, images from another cell, depolarized as indicated (mV, ms). The colour code marking regions and averaged fluorescence traces is the same as in Fig. 6. The star in *Bb* marks an infrequent discrete event that occurs superimposed with voltage-operated release.

**Table 1. Frequency of discrete events of $Ca^{2+}$ release**

| Fibre | Time | | Space | |
|---|---|---|---|---|
| | Rest | Pulse | Voltage insensitive | Voltage sensitive |
| 0118c | 2·38 | 1·34 | 5·59 | 0·73 |
| 0118e | 1·77 | 1·84 | 7·13 | 0·64 |
| 0128o | 0·99 | 3·09 | 2·63 | 0 |
| 0128p | 4·30 | 7·87 | 8·99 | 1·44 |
| 0128v | 5·68 | 7·35 | 2·13 | 0 |
| 0128w | 0·37 | 0·22 | 1·71 | 0·08 |
| 0310a* | 6·56 | 4·68 | 18·65 | 2·61 |
| 0310b* | 4·68 | 6·37 | 7·28 | 0 |
| Mean | 3·34 | 4·09 | 9·15 | 0·69 |
| S.E.M. | 0·81 | 1·03 | 2·52 | 0·33 |

* RyR3 knockout cells. Listed are frequency densities (expressed as $\times 10^{-3}\ \mu m^{-1}\ s^{-1}$) of discrete events in image regions separated either in time or space. Time was separated into 'pulse', meaning while depolarizing pulse was applied, or 'rest', all other times. Space was separated into regions where depolarization produced release (which is always continuous), 'voltage sensitive', and regions without response to voltage, 'voltage insensitive'.

release failed to take place at silent regions, regardless of the occurrence or timing of spontaneous events prior to the pulse. The frequency of events in these regions, $f_{V\text{insensitive}}$, was $1{\cdot}71 \times 10^{-3}\ \mu m^{-1}\ s^{-1}$, which was more than 20 times greater than $f_{V\text{sensitive}}$, $0{\cdot}08 \times 10^{-3}\ \mu m^{-1}\ s^{-1}$. When discrete $Ca^{2+}$ events were detected within the regions generating continuous release (Fig. 6*Ba*), they were completely uncorrelated with the applied pulse. The frequency of events at times before and after the depolarization, $f_{\text{rest}}$, was $0{\cdot}37 \times 10^{-3}\ \mu m^{-1}\ s^{-1}$ and was not significantly different from that during depolarization, $f_{\text{pulse}}$, $0{\cdot}22 \times 10^{-3}\ \mu m^{-1}\ s^{-1}$. This indicates that although two types of release were occasionally detected in the same confocal spot, they occurred independently. They may have originated from separate physical spaces within the confocal slice.

Very few discrete $Ca^{2+}$ release events were found during voltage clamp depolarization in RyR3-knockout myotubes (11 cells). They were also separate in space from voltage-induced $Ca^{2+}$ release, and occurred without correlation with the applied depolarization. Figure 7 shows examples from two cells. In Fig. 7*A* are two images scanned at the same line. The region where discrete $Ca^{2+}$ events occurred (red arrowhead and traces) did not release $Ca^{2+}$ upon depolarization. Regions indicated by black bars produced only continuous voltage-induced release (black trace). Figure 7*B* shows line-scans at two positions in another cell. In this and four other RyR3 knockout myotubes, discrete $Ca^{2+}$ events occurred chiefly at locations separated from those releasing $Ca^{2+}$ upon depolarization (Fig. 7*Ba*). When they coincided with continuous release, they occurred without any correlation with the applied pulse (Fig. 7*Bb*). The site marked by the red arrowhead in Fig. 7*Bb* generated discrete events before, during (marked by star) and after the depolarizing pulse.

Table 1 summarizes data obtained in eight experiments with wild-type and RyR3-knockout myotubes. On average, the frequency of $Ca^{2+}$ events at locations that did not produce continuous $Ca^{2+}$ release during depolarization ($f_{V\text{insensitive}}$, $(9{\cdot}15 \pm 2{\cdot}52) \times 10^{-3}\ \mu m^{-1}\ s^{-1}$) was almost 13 times greater than at places that released $Ca^{2+}$ upon depolarization ($f_{V\text{sensitive}}$, $(0{\cdot}69 \pm 0{\cdot}33) \times 10^{-3}\ \mu m^{-1}\ s^{-1}$), and their occurrence did not correlate with depolarization ($f_{\text{rest}}$, $(3{\cdot}34 \pm 0{\cdot}81) \times 10^{-3}\ \mu m^{-1}\ s^{-1}$ *vs.* $f_{\text{pulse}}$, $(4{\cdot}09 \pm 1{\cdot}03) \times 10^{-3}\ \mu m^{-1}\ s^{-1}$).

In summary, a voltage controlled and a spontaneous form of release coexist in developing myotubes (knockout or wild-type). One is continuous, the other is discrete, and their sources appear to be separate.

## DISCUSSION

The present study reveals that two locally different forms of $Ca^{2+}$ release coexist in developing mammalian muscle. One consists in discrete $Ca^{2+}$ release events, resembling to some extent $Ca^{2+}$ sparks found in mammalian cardiac (Cheng *et al.* 1993), smooth (Nelson *et al.* 1995), and frog skeletal muscle (Tsugorka *et al.* 1995; Klein *et al.* 1996). Examples of propagating release and the increase in event frequency by caffeine suggest that, as in other muscle tissues, $Ca^{2+}$ is involved as mediator of these discrete events. The second form of release is continuous, without discrete events, and is elicited by depolarization. A similar diffuse release constitutes a minor fraction of the total in the frog

(Shirokova & Ríos, 1997) and most, if not all, of $Ca^{2+}$ release in adult mammalian skeletal muscle (Shirokova *et al.* 1998). We now show that in developing muscle the two forms of release coexist, but are segregated.

### A molecular hypothesis of control

These observations must be interpreted in view of current ideas about control of $Ca^{2+}$ release. In skeletal muscle, alternating RyRs in double rows along the T tubule–SR junctions face DHPR tetrads (Franzini-Armstrong & Jorgensen, 1994) and are activated directly by voltage (Nakai *et al.* 1996). Then, in the frog, this would lead to opening of neighbouring channels (Ríos & Pizarro, 1988; Klein *et al.* 1996) by CICR (Endo, 1977; Fabiato, 1984). In mammalian skeletal muscle, by contrast, it is believed that control by voltage is dominant (one example of the evidence is the RISC phenomenon, Suda & Penner, 1994) while CICR contributes less, or not at all, as evidenced for example by the absence (Shirokova *et al.* 1998) or scarcity of sparks (Conklin *et al.* 1999). These functional differences have a structural correlate in the presence of different RyR isoforms. Indeed, the approximately equal representation of two isoforms in the frog (Murayama & Ogawa, 1992), where sparks coexist with continuous release, is in contrast with the preponderance of RyR1 in the mammal (Marks *et al.* 1989; Takeshima *et al.* 1989). Additionally, developing mammalian myotubes, where there are two forms of $Ca^{2+}$ release, express two RyR isoforms, but RyR3 disappears in the adult (Tarroni *et al.* 1997). Finally, there is evidence from bilayer experiments that RyR3 is more sensitive to activation by $Ca^{2+}$ than RyR1 (Chen *et al.* 1997; Jeyakumar *et al.* 1998; but see Murayama *et al.* 1999 for a more qualified perspective). These structure–function correlations suggested a molecular hypothesis to explain the different forms of release in frogs and developing mammalian cells: that RyR3, or $\beta$-RyRs in frogs, are necessary for the production of discrete events (Shirokova *et al.* 1998). The idea is strengthened by the observation that, unlike RyR1, RyR3 receptors expressed in a myogenic cell line do not induce the characteristic spatial arrangement of DHPRs in tetrads (Protasi *et al.* 1999) and hence are unlikely to establish the contact with them that is needed for direct control. It is also consistent with the report of spark-like events in the same cell line when RyR3 is expressed, and their absence upon the sole expression of RyR1 (Ward *et al.* 1999).

### Spatial segregation of two forms of $Ca^{2+}$ release

Observing mammalian cells in development, we now find something unexpected, and inconsistent with the molecular hypothesis as formulated above, that discrete events and voltage-operated release are strictly segregated, in spatially separated patches. In an urban metaphor, the type of activity is subject to zoning codes, which seem to be rigorously enforced.

In view of these results, the molecular hypothesis could be upheld if the supply of isoforms was patchy, restricted to some neighbourhoods of the cell, so that the ultimate determinant of the type of activity would still be the locally available isoform. The knockout experiments rule out this possibility, however: when only RyR1 is available the same two types of activity are observed, with a similarly segregated territorial distribution. It must be concluded that both isoforms are capable of producing discrete $Ca^{2+}$ events, but there is an intrinsic incompatibility between the two forms of control, resulting in suppression of discrete events whenever control by voltage is functionally in place. The determination of the type of activity appears to be supramolecular, rather than simply determined by the isoform type.

How could this exclusion work? It is reasonable that the direct interaction between sensors and release channels may 'take over' and impede other forms of activation, much in the same way as ryanodine-bound channels become impervious to other influences. To account for the absence of sparks this inhibition must also affect the intervening RyRs within the double row. This is plausible in multi-channel models of sparks, like the couplon of Stern *et al.* (1997), where inhibition emerges naturally as the 'cooling' effect of interspersing $Ca^{2+}$-insensitive channels within an array of $Ca^{2+}$-sensitive ones.

The situation in the mammal is in sharp contrast with frog muscle, where both forms of release are present, but no segregation is seen at the 0·5 $\mu$m scale of confocal resolution. The functional difference could depend on the structure of the DHPRs (Tanabe *et al.* 1987), which is different in frog muscle (Zhou *et al.* 1998). However, the interaction that excludes discrete events in the mammal cannot be the one that functions in release activation, because caffeine-stimulated rat cells with voltage sensors inactivated by depolarization still release $Ca^{2+}$ without discrete events (Shirokova *et al.* 1998). On the other hand, the basal inhibitory influence, exerted through a different region of the sensor (El-Hayek *et al.* 1995) might prevent spark activation in the mammal.

The above explanations invoke class-specific differences in the interactions between molecules. A more parsimonious one relies on the observation that RyR3 isoforms (analogous to amphibian $\beta$) do not establish connections with DHPRs (Protasi *et al.* 1999). Sparks might arise at junctional groups of channels where the regular connection with DHPRs is missing. Such hypothetical groups should be small (because in frog muscle there is no resolvable 'zoning' as in mammalian myotubes), and constituted mainly by $\beta$ RyRs (to explain the missing connections). The hypothesis is consistent with the stoichiometry of RyRs to DHPRs, greater in frog than in mammalian muscle (reviewed by Shirokova *et al.* 1996). It is also unifying, picturing spark-generating regions similar to cardiac junctions, devoid of directly connected voltage sensors (Sun *et al.* 1995).

### Role of RyR3 in $Ca^{2+}$ release

Because RyR3s do not couple structurally with voltage sensors (Protasi *et al.* 1999) their disappearance during development may be functionally important, allowing the

interaction with voltage sensors (and RyR1) to be established everywhere, and ultimately leading to the absence of $Ca^{2+}$ sparks in the adult mammalian muscle.

What is their role when they are present? The spontaneous events detected in cells lacking RyR3 had a substantially greater duration than those recorded in wild-type cells. Given that RyR3 channels in bilayers are less susceptible than RyR1 to $Ca^{2+}$ inactivation (Chen *et al.* 1997), this difference is surprising. If termination of discrete $Ca^{2+}$ release events, characterized in cardiac muscle as an inactivation (Sham *et al.* 1998), involved the '$Ca^{2+}$ inactivation' site probed by the bilayer experiments, one would expect longer-lasting events in wild-type, rather than in RyR3 knockouts. Alternatively, sideways 'allosteric' interactions between RyRs (Marx *et al.* 1998; Stern *et al.* 1999) might alter individual $Ca^{2+}$ release channels, depending on the type of RyRs in contact. In this context, one can speculate that RyR3s facilitate inactivation of RyR1 channels, thus making spontaneous events briefer in wild-type myotubes. Detailed structural data on isoform distribution would be useful to challenge such interaction hypotheses.

The absence of the RyR3 isoform does not seem to affect depolarization-induced $Ca^{2+}$ release in developing muscle (see also Dietze *et al.* 1998), and therefore is unlikely to influence its contractile properties. However, RyR3 receptors still may play a significant role in long-term $Ca^{2+}$ homeostasis, regulation of gene expression or other roles that require or depend on the production of discrete events not determined by voltage.

The finding that continuous and discrete forms of release originate at separate $Ca^{2+}$ sources indirectly supports a sequential model of triad formation (Flucher & Franzini-Armstrong, 1996). Indeed, our results suggest the transient existence of arrays of RyRs without voltage sensors, which is consistent with the proposal that formation of RyR arrays precedes the assembly of DHPR tetrads, resulting in junctions that transiently lack the full complement of voltage sensors.

Finally, the present results (and those of Conklin *et al.* 1999) are relevant to the nomenclature of discrete events. In adult heart and especially in frog skeletal muscle, discrete events, termed $Ca^{2+}$ sparks, are quite uniform in their spatial and temporal characteristics. In developing muscle, as shown here, the morphology is much more variable. A distinction between 'sparks' (those events that are brief and narrow) and wider, longer-lasting 'puffs', could be useful. However, we did not find in the distributions of width or duration a discontinuity that could provide a defining separation of such classes. We are left with the notion, similar to that in heart (Lipp & Niggli, 1996) and Ins$P_3$-mediated release in *Xenopus* oocytes (Sun *et al.* 1998) or HeLa cells (Bootman *et al.* 1997), of the existence in myotubes of a continuum of events, produced by different numbers of RyRs and controlled in different ways.


Beam, K. G. & Knudson, C. M. (1988). Calcium currents in embryonic and neonatal mammalian skeletal muscle. *Journal of General Physiology* **91**, 781–798.

Bertocchini, F., Ovitt, C. E., Conti, A., Barone, V., Scholer, H. R., Bottinelli, R., Reggiani, C. & Sorrentino, V. (1997). Requirement for the ryanodine receptor type 3 for efficient contraction in neonatal skeletal muscles. *EMBO Journal* **16**, 6956–6963.

Blatter, L. A., Hüser, J. & Ríos, E. (1997). Sarcoplasmic reticulum $Ca^{2+}$ release flux underlying $Ca^{2+}$ sparks in cardiac muscle. *Proceedings of the National Academy of Sciences of the USA* **94**, 4176–4181.

Bootman, M., Niggli, E., Berridge, M. & Lipp, P. (1997). Imaging the hierarchical $Ca^{2+}$ signalling system in HeLa cells. *Journal of Physiology* **499**, 307–314.

Chen, S. W., Li, X., Ebisawa, K. & Zhang, L. (1997). Functional characterization of the recombinant type 3 $Ca^{2+}$ release channel (ryanodine receptor) expressed in HEK293 cells. *Journal of Biological Chemistry* **272**, 24234–24246.

Cheng, H., Lederer, W. J. & Cannell, M. B. (1993). Calcium sparks: elementary events underlying excitation–contraction coupling in heart muscle. *Science* **262**, 740–744.

Cheng, H., Lederer, M. R., Lederer, W. J. & Cannell, M. B. (1996). Calcium sparks and $[Ca^{2+}]_i$ waves in cardiac myocytes. *American Journal of Physiology* **270**, C148–159.

Cheng, H., Song, L. S., Shirokova, N., González, A., Lakatta, E. G., Ríos, E. & Stern, M. D. (1999). Amplitude distribution of calcium sparks in confocal images. Theory and studies with an automatic detection method. *Biophysical Journal* **76**, 606–617.

Conklin, M. W., Powers, P., Gregg, R. & Coronado, R. (1999). $Ca^{2+}$ sparks in embryonic mouse skeletal muscle selectively deficient in dihydropyridine receptor $\alpha_{1S}$ or $\beta_{1a}$ subunits. *Biophysical Journal* **76**, 657–669.

Dietze, B., Bertocchini, F., Barone, V., Struk, A., Sorrentino, V. & Melzer, W. (1998). Voltage-controlled $Ca^{2+}$ release in normal and ryanodine receptor type 3 (RyR3)-deficient mouse myotubes. *Journal of Physiology* **513**, 3–9.

El-Hayek, R., Antoniu, B., Wang, J., Hamilton, S. L. & Ikemoto, N. (1995). Identification of calcium release-triggering and blocking regions of the II–III loop of the skeletal muscle dihydropyridine receptor. *Journal of Biological Chemistry* **270**, 22116–22118.

Endo, M. (1977). Calcium release from the sarcoplasmic reticulum. *Physiological Reviews* **57**, 71–108.

Fabiato, A. (1984). Dependence of the $Ca^{2+}$-induced release from the sarcoplasmic reticulum of skinned skeletal muscle fibres from the frog semitendinosus on the rate of change of free $Ca^{2+}$ concentration at the outer surface of the sarcoplasmic reticulum. *Journal of Physiology* **353**, 56*P*.

Flucher, B. E., Andrews, S. B. & Daniels, M. P. (1994). Molecular organization of transverse tubule/sarcoplasmic reticulum junctions during development of excitation-contraction coupling in skeletal muscle. *Molecular Biology of the Cell* **5**, 1105–1118.

Flucher, B. E. & Franzini-Armstrong, C. (1996). Formation of junctions involved in excitation-contraction coupling in skeletal and cardiac muscle. *Proceedings of the National Academy of Sciences of the USA* **93**, 8101–8106.

Franzini-Armstrong, C. & Jorgensen, A. O. (1994). Structure and development of E–C coupling units in skeletal muscle. *Annual Review of Physiology* **56**, 509–534.

González, A., Shirokova, N., Kirsch, W. G. & Ríos, E. (1999). Voltage and caffeine increase $Ca^{2+}$ spark amplitude in skeletal muscle. *Biophysical Journal* **76**, A385.

Herrmann-Frank, A., Lüttgau, H.-C. & Stephenson, D. G. (1999). Caffeine and excitation–contraction coupling in skeletal muscle: a stimulating story. *Journal of Muscle Research and Cell Motility* **20**, 223–237.

Jaimovich, E. & Liberona, J. L. (1997). Nuclear $IP_3$ receptors and calcium signals in cultured skeletal myotubes. *Biophysical Journal* **72**, A120.

Jeyakumar, L. H., Copello, J. A., O'Malley, A. M., Wu, G. M., Grassucci, R., Wagenknecht, T. & Fleischer, S. (1998). Purification and characterization of ryanodine receptor 3 from mammalian tissue. *Journal of Biological Chemistry* **273**, 16011–16020.

Klein, M. G., Cheng, H., Santana, L. F., Jiang, Y. H., Lederer, W. J. & Schneider, M. F. (1996). Two mechanisms of quantized calcium release in skeletal muscle. *Nature* **379**, 455–458.

Lechleiter, J. D. & Clapham, D. E. (1992). Spiral waves and intracellular calcium signalling. *Journal de Physiologie* **86**, 123–128.

Lipp, P. & Niggli, E. (1996). Submicroscopic calcium signals as fundamental events of excitation–contraction coupling in guinea-pig cardiac myocytes. *Journal of Physiology* **492**, 31–38.

Marks, A. R., Tempst, P., Hwang, K. S., Taubman, M. B., Inui, M., Chadwick, C., Fleisher, S. & Nadal-Ginard, B. (1989). Molecular cloning and characterization of the ryanodine receptor/junctional channel complex cDNA from skeletal muscle sarcoplasmic reticulum. *Proceedings of the National Academy of Sciences of the USA* **86**, 8683–8687.

Marx, S. O., Ondrias, K. & Marks, A. R. (1998). Coupled gating between individual skeletal muscle Ca release channels (ryanodine receptors). *Science* **281**, 818–821.

Murayama, T., Oba, T., Katayama, E., Oyamada, H., Oguchi, K., Kobayashi, M., Otsuka, K. & Ogawa, Y. (1999). Further characterization of the type 3 ryanodine receptor (RyR3) purified from rabbit diaphragm. *Journal of Biological Chemistry* **274**, 17297–17308.

Murayama, T. & Ogawa, Y. (1992). Purification and characterization of two ryanodine-binding protein isoforms from sarcoplasmic reticulum of bullfrog skeletal muscle. *Journal of Biochemistry* **112**, 514–522.

Nakai, J., Dirksen, R. T., Nguyen, H. T., Pessah, I. N., Beam, K. G. & Allen, P. D. (1996). Enhanced dihydropyridine receptor channel activity in the presence of ryanodine receptor. *Nature* **380**, 72–75.

Nelson, M. T., Cheng, H., Rubart, M., Santana, L. F., Bonev, A. D., Knot, H. J. & Lederer W. J. (1995). Relaxation of arterial smooth muscle by calcium sparks. *Science* **270**, 633–637.

Ogawa, Y., Kurebayashi, N. & Murayama, T. (1999). Ryanodine receptor isoforms in excitation-contraction coupling. *Advances in Biophysics* **36**, 27–64.

Parker, I., Zang, W. J. & Wier, W. G. (1996). $Ca^{2+}$ sparks involving multiple $Ca^{2+}$ release sites along Z-lines in rat heart cells. *Journal of Physiology* **497**, 31–38.

Percival, A. L., Williams, A. J., Kenyon, J. L., Grinsell, M. M., Airey, J. A. & Sutko, J. L. (1994). Chicken skeletal muscle ryanodine receptor isoforms: ion channel properties. *Biophysical Journal* **67**, 1834–1850.

Protasi, F., Takekura, H., Wang, Y., Chen, C. R. W., Franzini, A. C. & Allen, P. D. (1999). RyR3 expression in a dyspedic cell line does not restore junctional DHPr-tetrads. *Biophysical Journal* **76**, A470.

Ríos, E. & Pizarro, G. (1988). Voltage sensors and calcium channels of excitation-contraction coupling. *News in Physiological Sciences* **3**, 223–227.

Ríos, E., Stern, M. D., González, A., Pizarro, G. & Shirokova, N. (1999). Calcium release flux underlying $Ca^{2+}$ sparks of frog skeletal muscle. *Journal of General Physiology* **114**, 31–48.

Rousseau, E., Ladine, J., Liu, Q. Y. & Meissner, G. (1988). Activation of the $Ca^{2+}$ release channel of skeletal muscle sarcoplasmic reticulum by caffeine and related compounds. *Archives of Biochemistry and Biophysics* **267**, 75–86.

Sham, J. S., Song, L. S., Chen, Y., Deng, L. H., Stern, M. D., Lakatta, E. G. & Cheng, H. (1998). Termination of $Ca^{2+}$ release by a local inactivation of ryanodine receptors in cardiac myocytes. *Proceedings of the National Academy of Sciences of the USA* **95**, 15096–15101.

Shirokova, N., García, J., Pizarro, G. & Ríos, E. (1996). $Ca^{2+}$ release from the sarcoplasmic reticulum compared in amphibian and mammalian skeletal muscle. *Journal of General Physiology* **107**, 1–18.

Shirokova, N., García, J. & Ríos, E. (1998). Local calcium release in mammalian muscle. *Journal of Physiology* **512**, 377–384.

Shirokova, N. & Ríos, E. (1997). Small event $Ca^{2+}$ release: a probable precursor of $Ca^{2+}$ sparks in frog skeletal muscle. *Journal of Physiology* **502**, 3–11.

Smith, G. D., Keizer, J. I., Stern, M. D., Lederer, W. G. & Cheng, H. (1998). A simple numerical model of calcium spark formation and detection in cardiac myocytes. *Biophysical Journal* **75**, 15–32.

Stern, M. D., Pizarro, G. & Ríos, E. (1997). Local control model of excitation–contraction coupling in skeletal muscle. *Journal of General Physiology* **110**, 415–440.

Stern, M. D., Song, L. S., Cheng, H., Sham, J. S., Yang, H. T., Boheler, K. R. & Ríos, E. (1999). Local control models of cardiac excitation–contraction coupling. A possible role for allosteric interactions between ryanodine receptors. *Journal of General Physiology* **113**, 469–489.

Suda, N. & Penner, R. (1994). Membrane repolarization stops caffeine-induced $Ca^{2+}$ release in skeletal muscle cells. *Proceedings of the National Academy of Sciences of the USA* **91**, 5725–5729.

Sun, X.-P., Callamaras, N., Marchant, J. S. & Parker, I. (1998). A continuum of $InsP_3$-mediated elementary $Ca^{2+}$ signalling events in *Xenopus* oocytes. *Journal of Physiology* **509**, 67–80.

Sun, X. H., Protasi, F., Takahashi, M., Takeshima, H., Ferguson, D. G. & Franzini-Armstrong, C. (1995). Molecular architecture of membranes involved in excitation–contraction coupling of cardiac muscle. *Journal of Cell Biology* **129**, 659–671.

Sutko, J. L. & Airey, J. A. (1996). Ryanodine receptor $Ca^{2+}$ release channels: does diversity in form equal diversity in function? *Physiological Reviews* **76**, 1027–1071.

Takeshima, H., Nishimura, S., Matsumoto, T., Ishida, H., Kangawa, K., Minamino, N., Matsuo, H., Ueda, M., Hanaoka, M., Hirose, T. & Numa, S. (1989). Primary structure and expression from complementary DNA of skeletal muscle ryanodine receptor. *Nature* **339**, 439–445.

Tanabe, T., Takeshima, H., Mikami, A., Flockerzi, V., Takahashi, H., Kangawa, K., Kojima, M., Matsuo, H., Hirose, T. & Numa, S. (1987). Primary structure of the receptor for calcium channel blockers from skeletal muscle. *Nature* **328**, 313–318.

Tarroni, P., Rossi, D., Conti, A. & Sorrentino, V. (1997). Expression of the ryanodine receptor type 3 calcium release channel during development and differentiation of mammalian skeletal muscle cells. *Journal of Biological Chemistry* **272**, 19808–19813.

Tsugorka, A., Ríos, E. & Blatter, L. A. (1995). Imaging elementary events of calcium release in skeletal muscle cells. *Science* **269**, 1723–1726.

Ward, C., Castillo, D., Protasi, F., Wang, Y., Chen, S., Schneider, M. F. & Allen, P. (1999). Expression of Ryr3, but not Ryr1 produces $Ca^{2+}$ sparks in dyspedic myotubes. *Biophysical Journal* **76**, A386.

Wier, W. G., Ter Keurs, H. E. D. J., Marban, E., Gao, G. & Balke, C. W. (1997). $Ca^{2+}$ 'sparks' and waves in intact ventricular muscle resolved by confocal imaging. *Circulation Research* **81**, 462–469.

Zhou, J., Cribbs, L., Yi, J., Shirokov, R., Perez-Reyes, E. & Ríos, E. (1998). Molecular cloning and functional expression of a skeletal muscle dihydropyridine receptor from *Rana catesbeiana*. *Journal of Biological Chemistry* **273**, 25503–25509.

**Acknowledgements**

We thank Drs Gonzalo Pizarro and Lothar Blatter for encouragement and stimulating discussions, and Eric Nelson for expert technical help. This project was supported by grants from NIH (R01-AR32808 to E.R., T32-HL07692-07 and R01-AR45690 to N.S.), AHA (Scientist Development Grant to R.S.), MDA (to J.G.), and by grants from Telethon 1151 and MURST (to V.S.).

**Corresponding author**

N. Shirokova: Department of Molecular Biophysics and Physiology, Rush University, 1750 W. Harrison Street, Chicago, IL 60612, USA.

Email: nshiroko@rush.edu

**Authors' permanent address**

N. Shirokova and R. Shirokov: A. A. Bogomoletz Institute of Physiology, Ukrainian National Academy of Sciences, Kiev, 252601 GSP, Ukraine.